

The Effect of the Shunt Conductance on Transmission Line Models

Alécio B. Fernandes ⁽¹⁾ Washington L. A. Neves ⁽¹⁾

Edson G. Costa ⁽¹⁾ Max N. Cavalcanti ⁽²⁾

⁽¹⁾Laboratório de Alta Tensão
Universidade Federal da Paraíba
Av. Aprígio Veloso, 882, Campina Grande, PB
58.109-970, Brazil

⁽²⁾ Companhia Hidroelétrica do São Francisco - CHESF
Subestação Campina Grande II
Sítio Velame, S/N, Três Irmãs, Campina Grande, PB
58.100.970, Brazil
maxnorat@chesf.gov.br

alecio@dee.ufpb.br, waneves@dee.ufpb.br, edson@dee.ufpb.br

Abstract – In this work, sensitivity studies were performed using the EMTP in order to show the effects of shunt conductances on the characteristic impedance and on the propagation function of overhead transmission lines. Time domain simulations were carried out using modal and phase-domain line models. It is shown that simulation results are very sensitive to shunt conductance values. Laboratory measurements were carried out to provide better estimations for overhead line shunt conductances. Different insulator types, arrangements, and voltage classes were considered in the measurements. The estimated values can be used as default values for overhead transmission lines in EMTP programs.

Keywords: Transmission Lines, Shunt Conductance, Modal-domain, Phase-domain, EMTP.

I. INTRODUCTION

An accurate transmission line model must take frequency-dependent parameters into account. In frequency domain, a transmission line is completely characterized by the characteristic impedance and the propagation function [1]. These parameters are calculated from the line geometry and from conductors and ground resistivity data [2 - 7]. In several versions of the EMTP (Electromagnetic Transients Program) default values are assumed for the overhead lines shunt conductance [8 - 11]. The shunt conductance is considered to be a constant diagonal matrix, but the user is allowed to change its default values.

In this work, sensitivity studies were performed using ATP [10] and EMTDC [11] programs in order to show the effects of shunt conductances on the characteristic impedance and on the propagation function of overhead transmission lines. It is shown that the characteristic impedance, in the low frequency range, is very sensitive to shunt conductance changes whereas the propagation function remains the same. Time domain simulations for three-phase and double circuit three-phase transmission lines were carried out using transmission line modal-domain [1, 12] and phase-domain models [13 - 17].

Laboratory measurements using a high voltage Schering bridge were carried out to provide better estimations for overhead line shunt conductances considering different insulator types and arrangements.

Shunt conductances were estimated for glass, porcelain-type and non-ceramic insulators for 138 kV and 230 kV voltage classes. The estimated values can be used as default values for overhead transmission lines in EMTP type programs.

II. OVERHEAD LINE PARAMETERS

Consider an infinitesimal element with length dx of a single-phase transmission line, shown in Fig. 1.

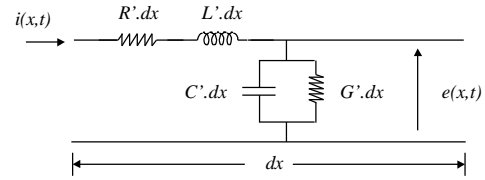


Fig. 1. Infinitesimal element of a single-phase transmission line.

In Fig. 1:

R' = resistance in Ω/km ;

L' = inductance in H/km ;

G' = shunt conductance in Ω^{-1}/km ;

C' = capacitance in F/km .

In multi-phase lines, the resistance R' is the result of the intrinsic conductors resistance plus the contribution of earth path resistance, both frequency-dependent. The inductance L' is also frequency-dependent, it is the result of the conductors inductance, earth path inductance and mutual inductance between phases.

The capacitance C' is nearly constant with frequency and depends on the line geometry. In EMTP programs, the shunt conductance G' is a diagonal matrix, whose values, g_{ii} , are defined for default, allowing for user changes. Default values are: $g_{ii} = 0.2 \cdot 10^{-9}$ mhos/km in FDDATA™ routine by MICROTRAN® [9]; $g_{ii} = 2.0 \cdot 10^{-9}$ mhos/km in LINE CONSTANTS routine by ATP [10]; and $g_{ii} = 1.0 \cdot 10^{-7}$ mhos/km in LINE CONSTANTS routine by EMTDC [11].

In summary, for a multi-phase line one could write:

$$\begin{aligned} Z'(\omega) &= Z'_{i-int}(\omega) + Z'_{ext}(\omega) + Z'_{earth}(\omega) \\ Y'(\omega) &= Y'_{ext}(\omega) \end{aligned} \quad (1)$$

where:

$Z'(\omega) = R'(\omega) + j \cdot \omega \cdot L'(\omega)$, serie impedance matrix;

$Y'(\omega) = G' + j \cdot \omega \cdot C'$, shunt admittance matrix;

$Z'_{i-int}(\omega)$ = intrinsic conductors impedance;

$Z'_{ext}(\omega)$ = geometric impedance;

$Z'_{earth}(\omega)$ = earth return path impedance;
 $Y'_{ext}(\omega)$ = geometric admittance.

III. CHARACTERISTIC IMPEDANCE AND PROPAGATION FUNCTION

Consider a multi-phase transmission line shown in Fig. 2.

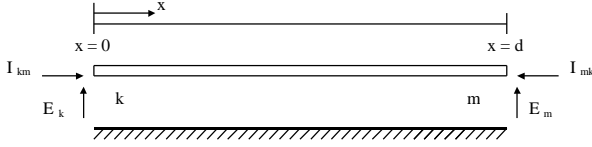


Fig. 2. Multi-phase transmission line.

Voltages and currents, in the frequency domain, must obey the following equations:

$$\begin{aligned} E_k(?) - Z_c(?) \cdot I_{km} (?) &= [E_m(?) + Z_c(?) \cdot I_{mk} (?)] \cdot A(?) \\ E_m(?) - Z_c(?) \cdot I_{mk} (?) &= [E_k(?) + Z_c(?) \cdot I_{km} (?)] \cdot A(?) \end{aligned} \quad (2)$$

where:

$Z_c(?) = Y' (?)^{-1} \cdot \sqrt{Y' (?) \cdot Z' (?)}$, characteristic impedance matrix;

$A(?) = e^{-\sqrt{Y' (?) \cdot Z' (?) \cdot d}$, propagation function matrix;

d = transmission line length;

$E(?)$ = voltage vector in the frequency domain;

$I(?)$ = current vector in the frequency domain.

The characteristic impedance (or admittance) and the propagation function characterize a transmission line completely.

IV. MODAL AND PHASE-DOMAIN MODELS

The solution of equation (2) can be found either by using Modal Transformation or by performing calculations directly in phase-domain.

Using the Modal Transformation [19] the “ n ” phases of a multiphase line can be decoupled in “ n ” single-phase lines. The modal characteristic impedance and modal propagation function are approximated by rational functions in the s plane [1]. $Z_c(\omega)$ and $A(\omega)$ are diagonal matrices. The transition from frequency domain to time domain is done directly without the use of inverse transformations. In time domain simulations, the voltages and currents in phase-domain are transformed to modal-domain and back to phase-domain again using Modal Transformation matrices. The modal-domain model is largely used and it is available in practically all EMTP programs [9 - 11].

Equation (2) can be solved directly in phase-domain [13 - 17]. The characteristic impedance and propagation function are approximated by rational functions in the phase-domain. Here, $Z_c(\omega)$ and $A(\omega)$ are full matrices. EMTP programs, like EMTDC and ATP have phase-domain models implemented [16, 17].

Modal models are accurate and efficient, but limited when applied to asymmetric lines, multi-circuit lines and underground cables. In these cases, phase-domain models had shown to be more accurate [13, 15, 16].

V. IMPLEMENTED ROUTINE

The authors implemented a routine to compute the line parameters. The program calculates $Z_c(\omega)$ and $A(\omega)$ in modal and phase-domain. All formulations proposed in [2 - 6] were implemented and the user can choose between them. It was validated through comparisons with LINE CONSTANTS routines of ATP and EMTDC results.

During the implementation and tests of the line parameters program the following questions came up: what are the default value to be chosen for the shunt conductance? How does the choice affect time-domain simulation results? Is a fixed shunt conductance value for all line configurations and voltage classes a good choice?

VI. SENSITIVITY ANALYSIS

The accuracy of a transmission line computational model depends on the fitting process to obtain rational functions in the modal-domain or in the phase-domain [12, 13, 16]. Sensitivity studies were performed using the EMTP in order to show the effects of shunt conductance on the characteristic impedance and on the propagation function of overhead transmission lines considering modal and phase-domain models.

A. Modal-Domain

Consider the three-phase untransposed transmission line shown in Fig. 3. Using LINE CONSTANTS ATP routine [10], $Z_c(\omega)$ and $A(\omega)$ were calculated in the frequency range from 10^{-2} Hz to 10^6 Hz for two chosen shunt conductance values: $2.0 \cdot 10^{-9}$ mhos/km (default value) and $1.0 \cdot 10^{-9}$ mhos/km (small absolute variation of default value). The results are shown in figs. 4 to 6.

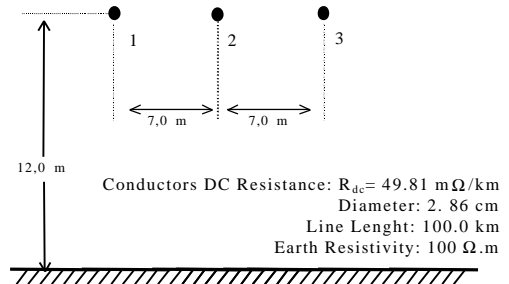


Fig. 3. Three-phase untransposed transmission line.

In the low frequency range, the magnitude and phase of the characteristic impedance are very sensitive to the shunt conductance value whereas the propagation function remains the same.

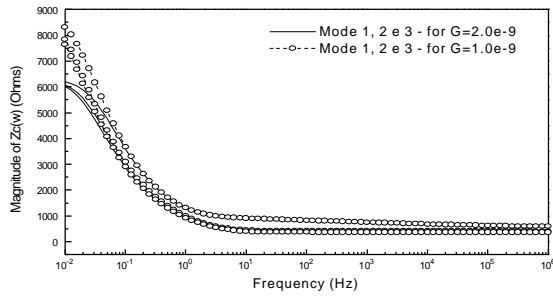


Fig. 4. Characteristic impedance magnitude – ATP – Shunt conductance values: $2.0 \cdot 10^{-9}$ and $1.0 \cdot 10^{-9}$ mhos/km.

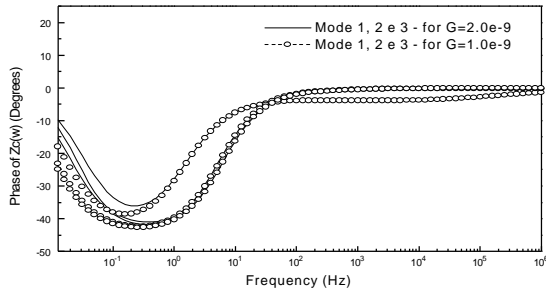


Fig. 5. Characteristic impedance phase – ATP – Shunt conductance values: $2.0 \cdot 10^{-9}$ and $1.0 \cdot 10^{-9}$ mhos/km.

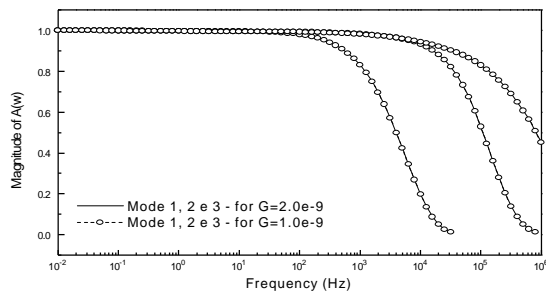


Fig. 6. Propagation function magnitude – ATP – Shunt conductance values: $2.0 \cdot 10^{-9}$ and $1.0 \cdot 10^{-9}$ mhos/km.

Using ATP, a step voltage of 1.0 p.u. was applied to phase 1, at the sending end, with the receiving end of phases 1, 2 and 3 left opened. The Modal Transformation matrix was calculated at 1.2 kHz and a $1.0 \mu\text{s}$ time step was used for the time domain simulation. The voltage waveforms at the receiving ends are shown in Fig. 7.

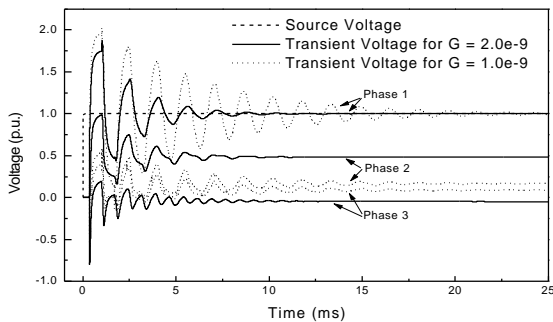


Fig. 7. Receiving end voltage waveforms – ATP – Shunt conductance values: $2.0 \cdot 10^{-9}$ and $1.0 \cdot 10^{-9}$ mhos/km.

It can be observed that small absolute changes in the shunt conductance values led to different results in time domain simulation.

B. Phase-Domain

Consider the three-phase double circuit overhead transmission line of Fig. 8.

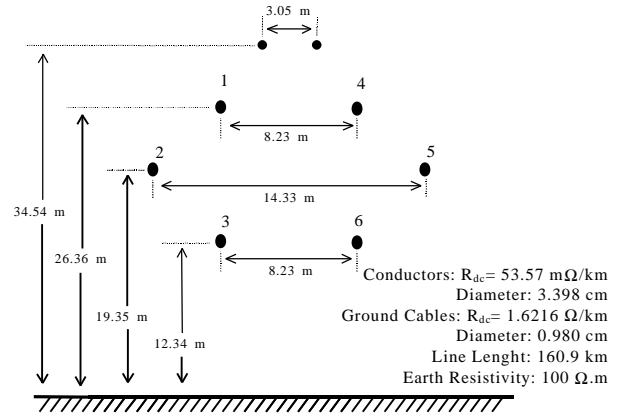


Fig. 8. Double-circuit with two parallel three-phase lines.

Using the line parameters program implemented by the authors, $Z_c(\omega)$ and $A(\omega)$ were calculated in the phase-domain in the frequency range from 10^{-2} Hz to 10^6 Hz, for three chosen shunt conductance values: $1.0 \cdot 10^{-9}$ mhos/km, $2.0 \cdot 10^{-9}$ mhos/km and $1.0 \cdot 10^{-8}$ mhos/km. The results are shown in figs. 9 to 11.

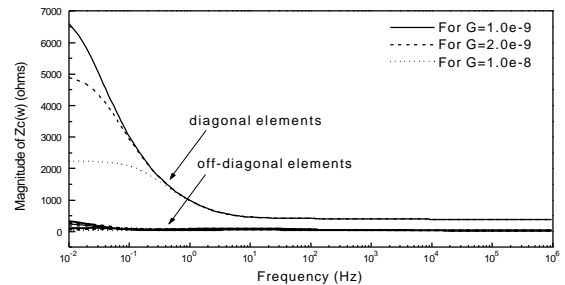


Fig. 9. Characteristic impedance magnitude – Elements of column 1 – Shunt conductance values: $1.0 \cdot 10^{-9}$, $2.0 \cdot 10^{-9}$ and $1.0 \cdot 10^{-8}$ mhos/km.

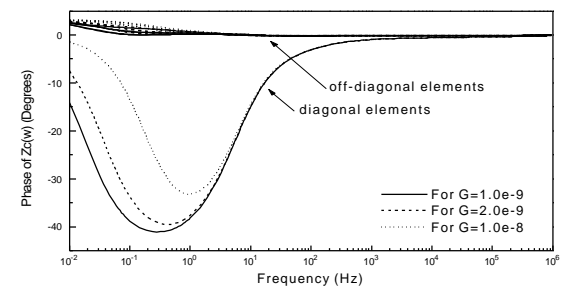


Fig. 10. Characteristic impedance phase – Elements of column 1 – Shunt conductance values: $1.0 \cdot 10^{-9}$, $2.0 \cdot 10^{-9}$ and $1.0 \cdot 10^{-8}$ mhos/km.

In the low frequency range, the magnitude and phase of the characteristic impedance matrix elements, especially the diagonal ones, are very sensitive to shunt

conductance values. As in the modal-domain, the propagation function in the phase-domain is not sensitive to the shunt conductance.

Using EMTDC, the transmission line of Fig. 8 was modelled in phase-domain. A step voltage of 1.0 p.u. was applied to phases 1, 2 and 3, at the sending end, with the receiving end of all phases left opened (Fig. 11). A 5.0 μ s time step was used for the time domain simulation. The voltage waveforms at the receiving ends (phases 4, 5 and 6, from 10 ms up to 100 ms) are shown in Fig. 12.

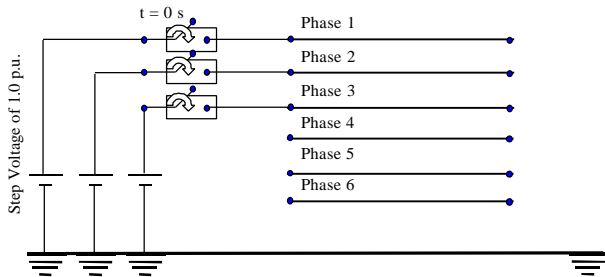


Fig. 11. A step voltage applied to phases 1, 2 and 3. All phases at the receiving end are opened.

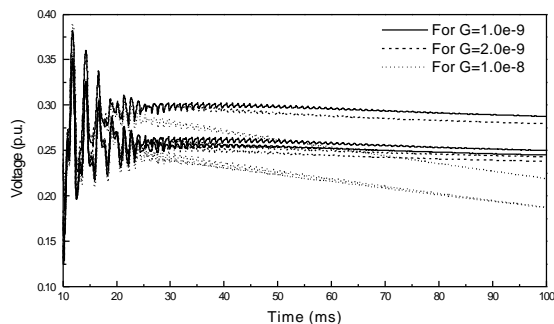


Fig. 12. Receiving end voltage waveforms at phases 4, 5 and 6 – EMTDC - Shunt conductance values: $1.0 \cdot 10^{-9}$, $2.0 \cdot 10^{-9}$ and $1.0 \cdot 10^{-8}$ mhos/km.

A positive sequence three-phase voltage (1.0 p.u. rms, 60 Hz) was applied to phases 1, 2 and 3 at the sending end, with the other terminals left opened. Fig. 13 shows the effect of the line trapped charges at the receiving ends (phases 1, 2 and 3) when the line is de-energized. A time step of 50.0 μ s was used for the time domain simulation.

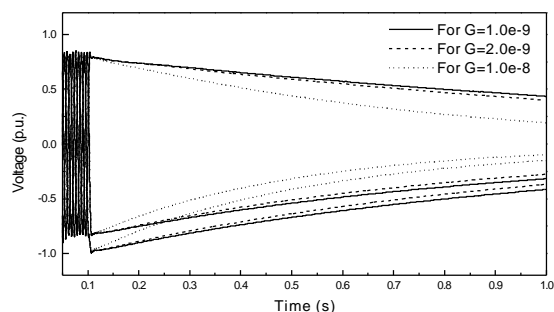


Fig. 13. Trapped charge voltages at phases 1, 2 and 3 – EMTDC - Shunt conductance values: $1.0 \cdot 10^{-9}$, $2.0 \cdot 10^{-9}$ and $1.0 \cdot 10^{-8}$ mhos/km.

Again, It can be observed that small absolute changes in the shunt conductance values led to different results in

time domain simulation.

There are many situations in which time-domain simulation results are not so sensitive to shunt conductance values. This is the case of a line-to-ground fault. The voltages at the receiving end of the line are not affected by the shunt conductances when a positive sequence voltage is applied to the sending end.

VII. LABORATORY MEASUREMENTS

In EMTP programs, the electric conduction through the air is neglected. Only the conduction through insulators is taken into account. So, shunt conductances are represented by a diagonal matrix.

Laboratory measurements were carried out to provide better estimations for overhead line shunt conductances. Two insulator configurations were used: with no grading shields and with grading shields. The following insulator types were considered:

- new glass-type insulators;
- old polluted glass-type insulators;
- new porcelain-type insulators;
- non-ceramic insulators.

A. Glass-type Insulators

Measurements were performed for 138 kV (a string of nine insulators) and 230 kV (a string of sixteen insulators) class of new and old (used) polluted glass-type insulators.

CHESF (Companhia Hidroelétrica do São Francisco) utility company supplied polluted insulators taken from an overhead line section near Natal, a Brazilian northeast city on the Atlantic coast. These insulators were used for more than 5 years and local pollution was preserved on their surfaces.

B. Porcelain-Type Insulators

Only new porcelain insulators were considered for 138 kV voltage class.

C. Non-ceramic Insulators

Two different non-ceramic insulators were considered for 138 kV: a Russian made insulator (insulator A) and a Brazilian made insulator (insulator B) largely used in the CHESF system.

For the 230 kV class a Brazilian made insulator (insulator C) was used.

D. Measured Results

Using a high-voltage Schering bridge, the insulator strings capacitance and their loss tangent were measured (Fig. 14) to determine the admittance parameters of Fig. 15. During the measurements the indoor temperature was in the range from 25°C to 27,5°C and the relative

humidity was in between 60% and 76%. The measured data are shown in tables 1 to 5.

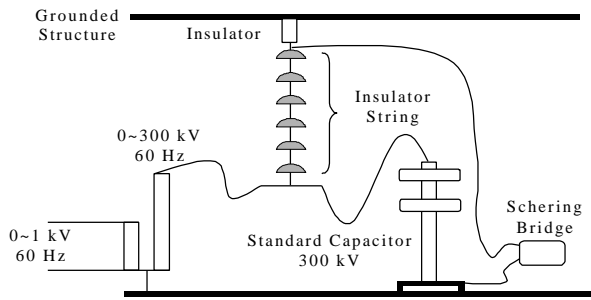


Fig. 14. Experimental set up: insulator string, standard capacitor and Schering bridge.

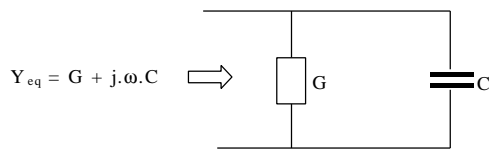


Fig. 15. Insulator string equivalent admittance.

Table 1 – Laboratory measurements – Glass-type insulators – 138 kV class (string of 09 insulators).

Applied Voltage 80 kV (rms)		Shunt Conductance (mhos)	Capacitance (pF)
New insulators	With no grading shields	1.6276×10^{-10}	16.0057
	With grading shields	1.9921×10^{-10}	21.0728
Polluted insulators	With no grading shields	8.0247×10^{-10}	19.2302
	With grading shields	9.2142×10^{-10}	23.6837

Table 2 – Laboratory measurements – Glass-type insulators – 230 kV class (string of 16 insulators).

Applied Voltage 133 kV (rms)		Shunt Conductance (mhos)	Capacitance (pF)
New insulators	With no grading shields	8.5816×10^{-11}	10.2638
	With grading shields	9.5276×10^{-11}	12.6487
Polluted insulators	With no grading shields	3.2433×10^{-10}	10.7509
	With grading shields	2.5231×10^{-10}	12.6163

Table 3 – Laboratory measurements – Porcelain-type insulators – 138 kV class (string of 09 insulators).

Applied Voltage 80 kV (rms)		Shunt Conductance (mhos)	Capacitance (pF)
New insulators	With no grading shields	1.6514×10^{-10}	14.6155
	With grading shields	1.8203×10^{-10}	19.3175

Table 4 – Laboratory measurements – Non-ceramic-type insulators – 138 kV class.

Applied Voltage 80 kV (rms)		Shunt Conductance (mhos)	Capacitance (pF)
Insulator A	With no grading shields	1.1964×10^{-12}	10.5889
	With grading shields	2.2427×10^{-12}	14.8868
Insulator B	With no grading shields	3.7525×10^{-13}	9.9636
	With grading shields	5.7766×10^{-13}	15.338

Table 5 – Laboratory measurements – Non-ceramic-type insulators – 230 kV class.

Applied Voltage 133 kV (rms)		Shunt Conductance (mhos)	Capacitance (pF)
Insulators C	With no grading shields	3.4256×10^{-11}	6.8906
	With grading shields	3.7927×10^{-13}	10.0702

Grading shields, pollution and ageing affect shunt conductance values.

For most configurations, conductance values increased a little bit when grading shields were used. Exceptions occurred for glass-type polluted insulator string and non-ceramic-type insulator, both for 230 kV class with no grading shields. In these situations, corona did appear affecting the measurements.

Shunt conductances are more sensitive to pollution and ageing. From tables 1 and 2 one can observe that shunt conductance values increased up to 4 times the new insulators conductance.

One should also notice that the higher the voltage class the smaller is the shunt conductance.

VIII. SHUNT CONDUCTANCE IN EMTP PROGRAMS

Considering an average of four towers per kilometer for a 138 kV overhead line (typical tower span of 250 m), the shunt conductance obtained from measurements was in the range from $1.5 \cdot 10^{-12}$ mhos/km (non-ceramic-type insulator) to $3.7 \cdot 10^{-9}$ mhos/km (glass-type polluted insulator string).

For a 230 kV line (typical tower span of 500 m), the shunt conductance was in the range from $7.6 \cdot 10^{-13}$ mhos/km (non-ceramic-type insulator) to $6.5 \cdot 10^{-9}$ mhos/km (glass-type polluted insulator string).

The measured results were close to MICROTRAN[®] and ATP default shunt conductance values for glass-type and porcelain-type insulators. For non-ceramic insulators, the measured shunt conductance values were much smaller than EMTP default values.

IX. CONCLUSIONS

The characteristic impedance, either in modal or phase-domain, is very sensitive to shunt conductance values in the low frequency range. This can affect time domain simulation results.

Laboratory measurements were carried out to determine appropriate shunt conductance values. Four different insulator types were used: new glass-type insulators, old polluted glass-type insulators, new porcelain-type insulators, and non-ceramic insulators. Insulator strings with no grading shields and with grading shields were considered for 138 kV and 230 kV voltage classes. Grading shields, pollution and ageing affect shunt conductance values.

Shunt conductance values obtained for glass-type and porcelain-type insulators were close to MICROTRAN[®] and ATP default values. For non-ceramic insulators, shunt conductance values were much smaller than the default values used in ATP, EMTDC and MICROTRAN[®] programs.

X. ACKNOWLEDGMENTS

The authors would like to thank the reviewers for their valuable suggestions, the High Voltage Laboratory / Electrical Engineering Department of UFPB, and CHESF for their support. The financial support of Mr. Alcécio B. Fernandes from the Brazilian National Research Council (CNPq) is gratefully acknowledged.

XI. REFERENCES

- [1] J. R. Marti, "Accurate Modelling of Frequency-Dependent Transmission Lines in Electromagnetic Transients Simulations", *IEEE Trans. Power Apparatus and Systems*, Vol. PAS-101, No.1, January, 1982, pp. 147-157.
- [2] J. R. Carson, "Wave Propagation in Overhead Wires with Ground Return", *Bell System Technical Journal*, Vol. 5, 1926, pp. 539-554.
- [3] A. Deri, G. Tevan, A. Semlyen, A. Castanheira, "The Complex Ground Return Plane, a Simplified Model for Homogeneous and Multi-Layer Earth Return", *IEEE Trans. Power Apparatus and Systems*, Vol. PAS-100, No. 8, August, 1981, pp. 3686-3693.
- [4] R. H. Galloway, W. B. Shorrocks, L. M. Wedepohl, "Calculation of Electrical Parameters for Short and Long Polyphase Transmission Lines", *Proc. IEE*, Vol. III, No. 12, December, 1964, pp. 2051-2059.
- [5] A. Semlyen, A. Deri, "Time Domain Modelling of Frequency Dependent Three-Phase Transmission Line Impedance", *IEEE Trans. on Power Apparatus and Systems*, Vol. PAS-104, No.6, June, 1985, pp.1549-1555.
- [6] L. M. Wedepohl, D. J. Wilcox, "Transient Analysis of Underground Power-Transmissions Systems: System-Model and Wave-Propagation Characteristics", *Proc. IEE*, Vol. 120, n°2, February, 1973, pp. 253-260.
- [7] M. B. Selak, J. R. Martí, H. W. Dommel, "Database of Power System Parameters for Data Validation in EMTP Studies: Overhead Transmission Line Application", *Proceedings of the 1999 International Conference on Power Systems Transients*, pp. 25-30, June 20-24, Budapest, Hungary.
- [8] H. W. Dommel, *Electromagnetic Transients Program Reference Manual*, Department of Electrical Engineering, The University of British Columbia, Vancouver, 1996.
- [9] Microtran Power System Analysis Corporation, *MICROTRAN - Transients Analysis Program Reference Manual*, Vancouver, 1992.
- [10] Leuven EMTP Center, *ATP - Alternative Transient Program - Rule Book*, Herverlee, Belgium, July, 1987.
- [11] Manitoba HVDC Research Center, *PSCAD/EMTDC Simulation Program - V3.0 Personal Edition*, Winnipeg, Canada, 2000.
- [12] A. B. Fernandes, W. L. A. Neves, "Frequency-Dependent Low Order Approximation of Transmission Line Parameters", *Proceedings of the 1999 International Conference on Power Systems Transients*, pp. 43-48, June 20-24, Budapest, Hungary.
- [13] F. Castellanos, J. R. Marti, "Full Frequency-Dependent Phase-Domain Transmission Line Parameters", *IEEE Transactions on Power Systems*, Vol.12, No.3, August, 1997, pp. 1331-1339 .
- [14] H. V. Nguyen, H. W. Dommel, J. R. Martí, "Direct Phase-Domain Modelling of Frequency-Dependent Overhead Transmission Lines", *IEEE Trans. on Power Delivery*, Vol. 12, No.3, July, 1997, pp. 1335-1342.
- [15] A. Morched, B. Gustavsen, M. Tartibi, "A Universal Model for Accurate Calculation of Electromagnetic Transients on Overhead Lines and Underground Cables", *IEEE Trans. on Power Delivery*, Vol. 14, Iss.3, July, 1999, pp. 1032-1038.
- [16] B. Gustavsen, G. Irwin, R. Mangelrod, D. Brandt, K. Kent, "Transmission Line Models for the Simulation of Interaction Phenomena between AC and DC Overhead Lines". *Proceedings of the 1999 International Conference on Power Systems Transients*, pp. 61-67, June 20-24, Budapest, Hungary.
- [17] T. Noda, N. Nagaoka, A. Ametani, "Further Improvements to a Phase-Domain ARMA Line Modeling Terms of Convolution, Steady-State Initialization, and Stability", *IEEE Trans. on Power Delivery*, Vol. 12, No.3, July, 1997, pp.1327-1334.
- [18] M. D'Amore, M. S. Sarto, "A New Formulation of Lossy Ground Return Parameters for Transient Analysis of Multiconductor Dissipative Lines", *IEEE Trans. on Power Delivery*, Vol. 12, No.1, January, 1997, pp.303-313.
- [19] L. M. Wedepohl, "Application of Matrix Methods to the Solution of Travelling-Wave Phenomena in Polyphase Systems", *Proc. IEE*, Vol. 110, n°12, December, 1963, pp. 2200-2212.